PHYSICAL REVIEW B VOLUME 23, NUMBER 2 15 JANUARY 1981

Photoconductivity, trapping, and recombination in discharge-produced, hydrogenated amorphous silicon

Christopher R. Wronski* and Ronald E. Daniel
R.C.A. Laboratories, Princeton, New Jersey 08540
(Received 9 October 1978; revised manuscript received 25 July 1980)

Photoconductivity, trapping, and recombination have been studied in undoped, hydrogenated amorphous silicon (a-SiH$_x$) films prepared by the discharge decomposition of silane. In this study the effects of the photoinduced, reversible conductivity changes have been taken into account in the characterization of the different types of electron trapping and recombination kinetics. These kinetics, which over the temperature range of $\sim$350 to 120 K are found to be consistent with free-carrier transport, are correlated with the densities, energies, and free-carrier capture cross sections of the states in the gap. The electron lifetimes, between $\sim 10^{-6}$ and 10^{-3} s, are shown to be dependent on two types of recombination centers located at or below midgap with one of these centers having an electron capture cross section, S_n, of $\sim 10^{-19}$ cm^2. The electron lifetimes are found to be sensitive to these centers even though their densities are $\lesssim 10^{-4}$ that of the hydrogen present in the films. The electron trapping is determined by the states above midgap, which have densities of $\sim 10^{17}$ cm^{-3} eV^{-1} over the energy range of $\sim$0.6 to 0.35 eV from the free electron band and for energies within $\sim$0.2 eV, densities of $\sim 10^{19}$ cm^{-3}. No evidence is found for a large peak in the densities of states at $\sim$0.4 eV from E_c, a peak which has been extensively reported for a-SiH$_x$ films.

INTRODUCTION

There is a large interest in the optical and electronic properties of undoped, but n-type, hydrogenated amorphous silicon (a-SiH$_x$) produced by the discharge decomposition of silane.[1-3] Such films deposited onto substrates at temperatures between ~200 and 300 °C have been extensively used in fabricating high-quality junctions[4,5] and efficient solar-cell structures.[6,7] A variety of methods[8,9,10] is being used to investigate the optical and electronic properties as well as the densities of gap states in these films. This includes studies of photoconductivity[11-13] which have been carried out on films deposited under a variety of different conditions. There are however, ambiguities associated with many of the results reported because in the majority of these studies no consideration had been given to the effects that thermal- and optical-exposure histories of the films have on the photoconductivities.[14,15] In this paper we present and characterize the photoconductivities of undoped rf and dc discharge produced a-SiH$_x$ films in which these effects are taken fully into account.

The reversible conductivity changes in the films studied were due to photoinduced changes in the properties of the bulk material[15,16] rather than to substrate-[17] and surface-adsorption[18] effects. Therefore the contribution of these conductivity changes to the bulk-photoconductivity characteristics could be accurately evaluated. In addition these changes could be utilized in significantly extending the range over which the photoconductivities could be studied in the *same* film. Thus the photoconductivities in these undoped films could be characterized for a range of electron quasi-Fermi levels between ~0.6 and 0.3 eV from the free carrier band and electron lifetimes from ~ 10^{-6} to 10^{-3} s. This range of photoconductivities was achieved without the serious perturbation in the gap states caused by the introduction of dopants.[13] The photoconductivities were obtained by changing the illumination levels and temperatures over the range from ~350 to 120 K. In agreement with previously reported junction and photovoltaic properties on similar films, the results obtained over this wide temperature range are consistent with free-carrier transport in the extended states. Such free-carrier transport allows the photoconductivities to be considered in terms of the electron trapping and recombination kinetics extensively treated by Rose.[19,20] These treatments, applied to results of photocurrent response times and electron lifetimes, are utilized in obtaining insights into the densities, energies and free-carrier capture cross sections of various states in the gap of the a-SiH$_x$ films.

EXPERIMENTAL PROCEDURE

The a-SiH$_x$ films were deposited by rf and dc discharge decomposition of silane onto fused quartz substrates at temperatures, T_s, between ~ 190 and 330 °C.[12] The photoconductivities of the ~ 1 μm thick undoped, but n-type films, were measured using coplanar metal-n^+ a-SiH$_x$ electrodes.[21] All the currents studied exhibited Ohmic behavior and the majority of the measurements were carried out with 100 V applied across electrodes 1 mm apart. The photoconductivities were measured on known and reproducible states of conductivity in

the films which were obtained by annealing the films at 200 °C in vacuum (annealed state) and subsequently subjecting them to known exposures of 200-mW/cm^2 white light (soaked state).[15,16] These controlled, reproducible dark and light conductivities were not affected by the illuminations used in the experiments.

The photocurrents were generated by monochromatic light having $\lambda = 0.61$ μm and intensities ranging from 1×10^{12} to 1×10^{15} photons cm^{-2} s^{-1}. In all cases the photocurrents were significantly greater than the dark currents and corresponded to uniform-carrier generation because the optical absorption of the films at $\lambda = 0.61$ μm is $\sim 2\times10^4$ cm^{-1}.[12] As a result the bulk photoconductivity σ_p could be obtained directly from the photocurrents and the known geometry, thickness, and electric fields. These photoconductivities were measured over the temperature range from ~350 to 120 K using a vacuum cryostat having a thermocouple in good thermal contact with the sample.

The steady-state photoconductivities and their dependence on the intensity of illumination and temperature were used to characterize the recombina- and the electron lifetimes. The free electron densities n and the electron lifetimes τ_n were obtained from the relations

$$\sigma_p = q\mu_n n \tag{1a}$$

and

$$n = f\tau_n , \tag{1b}$$

where q is the electronic charge, μ_n the microscopic mobility in the conduction band (extended states for electrons) and f is the volume-generation rate of free carriers. For 100% efficiency of free-electron-hole pair generation,[22] f is given by

$$f = F(1-R)[1-\exp(-\alpha d)]/d , \tag{2}$$

where F cm^{-2} s^{-1} is the incident photon flux, R is the surface reflection, α is the optical absorption coefficient, and d is the thickness of the film. The electron densities and lifetimes were calculated from Eqs. (1a) and (1b) using f and a value μ_n = 1 cm^2 V^{-1} s^{-1}. Although the electron mobilities in the extended states of a-SiH$_x$ have not been measured, the value of 1 cm^2 V^{-1}s^{-1} for the microscopic mobility is not inconsistent with the results obtained for the electron drift mobilities on similar films.[23]

The decays of steady-state photocurrents generated by different intensities of illumination were used to characterize electron trapping. These decays, obtained by terminating the illumination with a mechanical shutter, were characterized by the time taken for the photocurrents to decay to half their steady-state values, τ_0. These decay times. which were much longer than the electron lifetimes, are given by

$$\tau_0 = \left(1+\frac{n_t}{n}\right)\tau_n = \frac{n_t}{n}\tau_n , \tag{3}$$

where n_t is the density of trapped electrons emptied in the time τ_0. Because in all the cases studied the quasi-Fermi levels, E_{Fn}, was significantly displaced from the dark Fermi level n_t could be related to the densities of states acting as traps in the vicinity of E_{Fn}, $N_t(E_{Fn})$ cm^{-3} eV^{-1}, by $n_t = kT/qN_t(E_{Fn})$.[20] The positions of E_{Fn} relative to the conduction band E_c were obtained for the various values of σ_p and n using the relation

$$n = N_c \exp[-(E_c - E_{Fn})/kT] , \tag{4}$$

where N_c is the effective density of states at E_c. The value used for N_c was 10^{20} cm^{-3}, a value that is consistent with a $\mu_n = 1$ cm^2 V^{-1} s^{-1} and a $\mu_n N_c = 10^{20}$.[24]

EXPERIMENTAL RESULTS

The photoconductivities of the a-SiH$_x$ films studied exhibited a wide range of characteristics

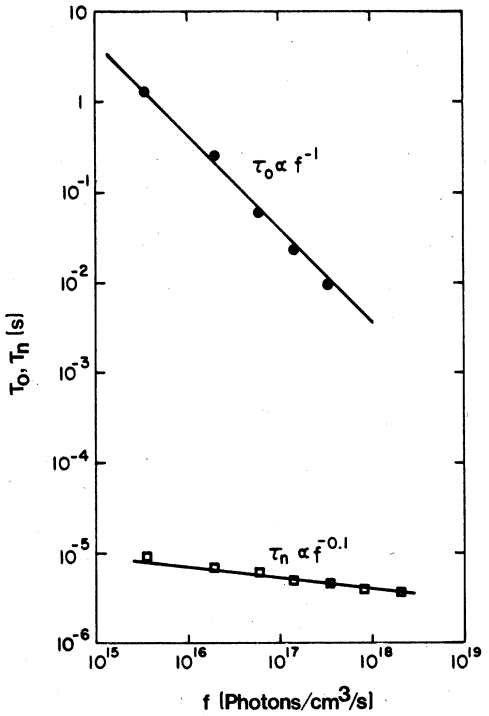

FIG. 1. Response time τ_0 and the electron lifetime τ_n plotted versus the photogeneration rate f. The results are for an rf discharge-produced film deposited at T_s = 320 °C after the film had been annealed at 200 °C and subsequently exposed to 200-mW/cm^2 illumination for four hours.

which depend on the fabrication conditions as well as the optical and thermal histories of the films. Example of the differences in the characteristics that can be obtained in the same film, due to reversible conductivity changes, are presented in Figs. 1 and 2 for an rf discharge-produced film deposited at $T_s = 300\,^{\circ}C$. Figure 1 shows the room-temperature τ_n and τ_0 as a function of f for the film after it had been annealed and then exposed to the 200-mW/cm^2 white light illumination for four hours. Figure 2 shows the room-temperature τ_n and τ_0, over the same range of f as in Fig. 1, for the film after it had been annealed and not subjected to any 200-mW/cm^2 illumination. These results, as well as those obtained on a large number of other films, indicate that the dependences of the photoconductivities and electron lifetimes on intensity of illuminations have the form

$$\sigma_p \propto f^{\gamma} \tag{5a}$$

and

$$\tau_n \propto f^{-(1-\gamma)}, \tag{5b}$$

where γ is a constant. The response times on the other hand exhibit dependences which can be quite closely related to the corresponding values of γ by

$$\tau_0 \propto f^{-\gamma}. \tag{6}$$

The results in Fig. 1 for the film in the "soaked" conductivity state correspond to a value of $\gamma = 0.9$. This is reflected in the insensitivity of τ_p to f and the position of E_{Fn}, where the values of τ_n, 8×10^{-6} to 5×10^{-6}, are virtually constant as $E_c - E_{Fn}$ changes from 0.55 to 0.45 eV. This is in contrast to τ_0, which decreases by two orders of magnitude, from ~1 to 1×10^{-2} s, and which exhibits a dependence $\tau_0 \propto f^{-1}$ in close agreement with Eq. (6). Even though τ_0 undergoes these large changes it is important to note that these characteristics correspond to an n_t, given by Eq. (3), which remains constant at 6×10^{15} cm^3 even though n increases from 7×10^{10} to 3×10^{12} cm^{-3}. In the case of the "annealed" film in Fig. 2 the values of τ_n and τ_0, shown for the same range of f as that of Fig. 1, exhibit characteristics which correspond to the value of $\gamma = 0.5$ and electron lifetimes which depend on the position of E_{Fn}. In Fig. 2 the electron lifetimes, which are significantly larger than those in Fig. 1, decrease from 1×10^{-3} to 1×10^{-4} s as $E_c - E_{Fn}$ changes from 0.38 to 0.3 eV. The corresponding values of τ_0 have a dependence $\tau_0 \propto f^{-0.54}$ which is completely different from that seen in Fig. 1, but which is again close to the relation given by Eq. (6). The characteristics seen in Fig. 2 yield a virtually constant ratio for τ_0/τ_n which reflects a continuous increase in n_t as $E_c - E_{Fn}$ decreases. The values of n_t increase

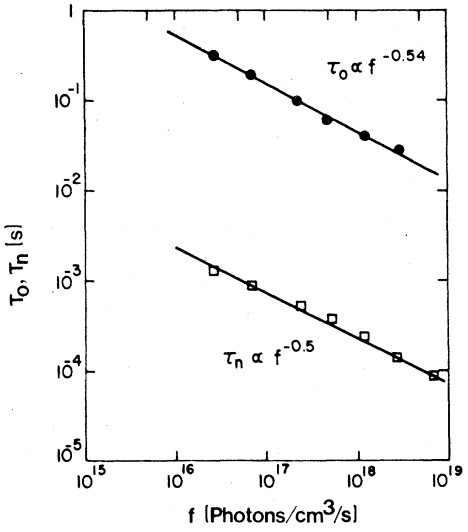

FIG. 2. Response time τ_0 and the electron lifetime τ_n versus the photogeneration rate f for the same rf film as in Fig. 1. The results here are for the film after an anneal at 200 °C and *no* subsequent exposure to the 200-mW/cm^2 illumination.

from 6×10^{15} cm^{-3} at $f \sim 10^{16}$ cm^{-3} s^{-1} to 2×10^{17} cm^{-3} at $f \sim 10^{19}$ cm^{-3} s^{-1}, thus becoming significantly greater than the constant n_t of 6×10^{15} cm^{-3} indicated by the results in Fig. 1 (although not shown in Fig. 2, the characterisitics of σ_p for $f < 10^{16}$ cm^{-3} s^{-1} were close to those shown in Fig. 1.)

The range of photoconductivity characteristics and the effect that the reversible conductivity changes can have both the photoconductivities as well as the values of γ, τ_0, and τ_n are clearly illustrated in Figs. 1 and 2. The values of γ that have been most commonly observed are $0.5 \leq \gamma \leq 1$, with the values significantly different from 0.5 and 1.0 being clearly not due to a mixture of monomolecular and bimolecular types of characteristics.[20] An example of a $\gamma = 0.7$ is shown in Fig. 3 where the τ_0 and τ_n characteristics, for a dc-discharge-produced film at $T_s = 300\,^{\circ}C$, are presented for the same range of f values as those in Figs. 1 and 2. The dependence of τ_n and τ_0 on f are again in good agreement with the relations indicated by Eqs. (5a), (5b), and 6, where τ_n changes from 3×10^{-4} to 5×10^{-5} s and τ_0 from 3×10^{-1} to 6×10^{-3} eV and the densities of trapped electrons n_t from 3×10^{15} to 8×10^{15} cm^{-3}. The large deviation of γ from unity is reflected by the significant changes in τ_n as $E_c - E_{Fn}$ decreases. However, it should be noted here that in contrast to the characteristics shown in Fig. 2 for $\gamma = 0.5$, the dependences of τ_0 and τ_n on f in Fig. 3 are completely different from each other. The above results of quite different types of recombination and trapping pro-

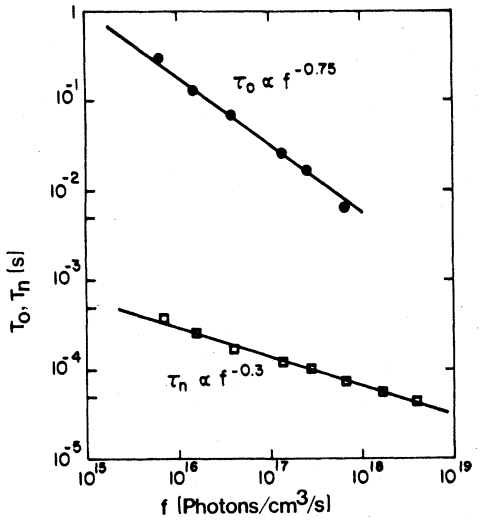

FIG. 3. Response time τ_0 and the electron lifetime τ_n as a function of photogeneration rate f for a dc discharge-produced film deposited at $T_s = 320$ °C (Ref. 21). These measurements were carried out on the film after only an anneal of 200 °C.

cesses in the a-SiH$_x$ films even in the *same* film at the *same* temperature, clearly reflect the effects resulting from different values of τ_n and positions of E_{Fn}. They also indicate (Fig. 2) that for E_{Fn} sufficiently close to E_c the densities of trapped electrons can exceed 10^{16} cm^{-3}. These values, which are comparable to the densities reported for states near midgap,[25,26] are obtained in a photoconductivity regime in which there is a striking similarity between the dependence of τ_n and τ_0 on f (and $E_c - E_{Fn}$). The ability to observe this regime however depends on the values of τ_n in the films since they determine the position of E_{Fn} for a given value of f.

In order to extend the range over which E_{Fn} could be moved with the values of f used, advantage was taken of the enhanced displacements that occur in E_{Fn} when the temperature is lowered. These displacements, given by Eqs. (1a), (1b), and 4, allow E_{Fn} to be moved over a large fraction of the gap for the same values of f. The effect of this on the photoconductivities, whose room-temperature characteristics are shown in Fig. 2, are presented in Fig. 4 where $\log_{10}(\sigma_p)$ is plotted versus $1/T$ for the temperature range of ~350 to 120 K. These results were obtained reproducibly during both the heating and cooling cycles of the experiments. The results in Fig. 4 include data obtained with $f < 10^{16}$ cm^{-3} s^{-1} which are not shown in Fig. 2 but, as indicated earlier, exhibited room-temperature characteristics similar to those shown in Fig. 1, i.e., $\gamma = 0.9$. The regimes of the two different photoconductivity characteristics are separated by the line signified as σ_{TR} in Fig. 2. On the left of this line the photoconductivity is virtually independent of temperature and σ_p has a $\gamma = 0.9$. In the other regime, where $\gamma = 0.5$, σ_p has an activation energy of ~0.1 eV (and subsequently ~0.2 eV). The transition from one regime to the other, accompanied by the change in γ, indicates a transformation of recombination and trapping kinetics from those illustrated in Fig. 1 to those illustrated in Fig. 2. The temperature independence of σ_p having $\gamma = 0.9$ reflects the independence of τ_n on f and hence E_{Fn} as in results shown in Fig. 1. The onset of a σ_p which is no longer temperature independent reflects a sufficiently small value of $E_c - E_{Fn}$ which changes the kinetics to those yielding a τ_n dependent on E_{Fn}. The requirement that E_{Fn} reach a certain position in the gap in order for this change in kinetics to occur is clearly indicated by the dependence of the transition temperatures on f. For the lower value of f the transitions occur at lower temperatures, since larger displacements of E_{Fn}

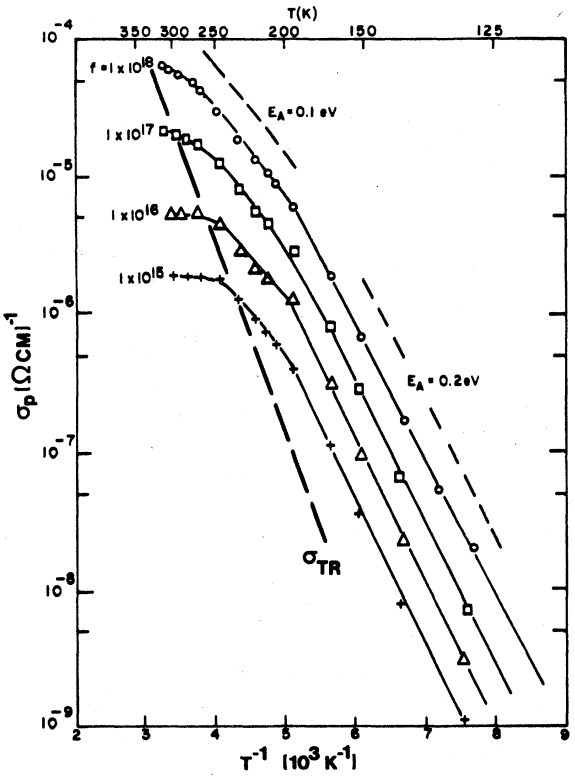

FIG. 4. Logarithm of photoconductivities versus the reciprocal of temperature at several levels of photogeneration rates. These results are for the rf discharge-produced film and photoconductivities whose room-temperature results are shown in Fig. 2. The photogeneration rates f shown are from 1×10^{15} to 1×10^{18} cm^{-3} s^{-1}.

are required from their room-temperature values. This results in a temperature-dependent σ_{TR}, seen in Fig. 3, which has an activation energy of ~0.2 eV.

Although at the lowest temperatures studied there is an additional transition in σ_p, which is also dependent on f and is accompanied by a change in γ from 0.5 to ~0.4, this transition could not be readily characterized because of the small changes in γ. However, it is noteworthy that it corresponds to changes in activation energies from ~0.1 to 0.2 eV so that all the transitions in Fig. 4 reflect changes to higher activation energies at lower temperatures. These results are in direct contrast to those of Spear, Loveland, and Al-Shabarty[11] who reported transitions for σ_p into $\gamma = 0.5$ regimes which had very low activation energies at the lower temperatures and transitions which were both independent of f as well as always occuring at the *same* temperature. These authors explained the results by the onset of hopping conductivity in the $\gamma = 0.5$ regimes. As will be shown later the results reported here are not only consistent with free-carrier transport in all the photoconductivity regimes, but also with the recombination and trapping kinetics indicated by room-temperature characteristics.

The temperature dependence of σ_p exhibiting $\gamma = 0.7$ at room temperature has been reported by Wronski and Carlson.[21] These photoconductivities also exhibit f-dependent transitions from regions of $\gamma = 0.7$, which have activation energies significantly less than 0.1 eV to regions of $\gamma = 0.5$ with activation energies ~0.1 eV. The small but clearly detectable activation energies of the $\gamma = 0.7$ regimes are consistent with the recombination and trapping kinetics of such photoconductivities. However, these activation energies result in transitions between the two regimes which cannot be as readily analyzed on a $\log_{10}(\sigma_p)$ versus $1/T$ plots as those corresponding to γ close to unity (Fig. 4). Results of an alternative method of analysis are presented in Fig. 5 for the transitions of σ_p having $\gamma = 0.83$. This γ is still significantly different from unity but results in a smaller activation energy for σ_p than a $\gamma = 0.7$. The results in Fig. 5 were obtained on the same rf film as the one whose characteristics are shown in Fig. 1 to Fig. 3, but now the photoconductivities were obtained after the film was annealed and exposed to the standard illumination for two hours, half the time used in the case of Fig. 1. At room temperature the photoconductivity had a $\gamma = 0.83$ over the entire range of f, up to the maximum of 2×10^{19} $cm^{-3}\,s^{-1}$. However, as the temperature was lowered, transitions to a regime of $\gamma = 0.5$ and activation energies of ~0.1 eV were obtained. The

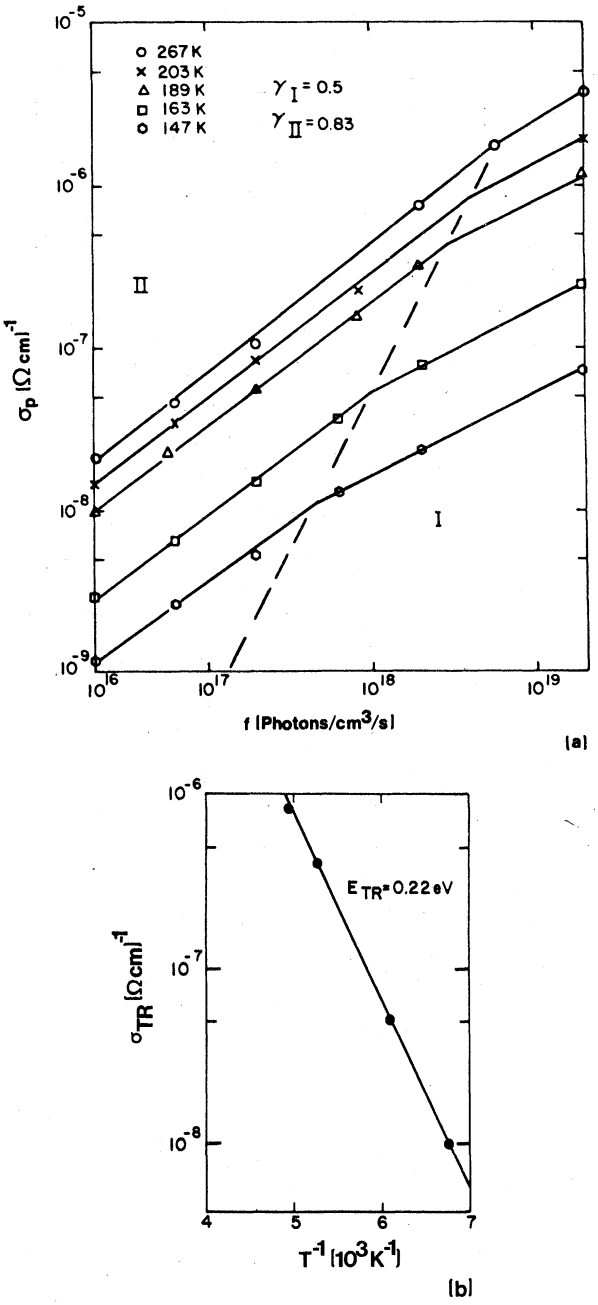

FIG. 5. (a) Dependence of the photoconductivity on the photogeneration rate at several temperatures. (b) Plot of the logarithm of photoconductivity at the transition point of (a) versus the inverse of the temperature. These measurements were carried out on the rf discharge-produced film deposited at $T_s = 320$ °C after an anneal of 200 °C and an exposure to the 200-mW/cm^2 illumination for two hours.

transitions exhibit dependences on f and T which are similar to those reported for $\gamma = 0.7$.[21] The dependence that σ_p has on f at differnt tempera-

tures is shown in Fig. 5(a) where the experimental points are divided into the two regimes, $\gamma_I = 0.83$ and $\gamma_{II} = 0.5$ by the dashed line. This dashed line corresponds to transition conductivities σ_{TR}, similar to those seen in Fig. 3. The values of $\log_{10}(\sigma_{TR})$ versus $1/T$ are plotted in Fig. 5(b) and the activation energy that is obtained for σ_{TR} is $E_{TR} = 0.22$ eV, a value in good agreement with that observed in Fig. 3. It is also important to note that these values of E_{TR}, are close to twice that of the activation energy of ~0.1 eV found for the regimes having $\gamma = 0.5$.

DISCUSSION OF RESULTS

The recombination and trapping kinetics extensively treated by Rose are applied here to the photoconductivity characteristics described in the preceding section. These results, as well as those reported elsewhere[12,15,21,27] for the photoconductivities of similar films are correlated with a continuous distribution of gap states shown schematically in Fig. 6. The distribution of Fig. 6 is subdivided into four energy regions because such a division is useful in relating the photoconductivity not only to the densities and carrier capture cross sections of the various states but also to their energies relative to the free-carrier bands, E_c and E_v. The large densities of states observed in drift mobility measurements are represented by the two regions $E_c - E_{tn}$ and $E_{tp} - E_v$, with densities N_{tn} and N_{tp}. Although these regions cannot be precisely defined they are associated with values of $E_c - E_{tn} \sim 0.2$ eV and $E_{tp} - E_v \sim 0.3$ to indicated by drift mobility[23] as well as the previously published photoconductivity results.[21,27] The deeper lying states are divided into two classes, identified by subscripts 1 and 2, where the dividing line is placed at approximately midgap. For convenience the states classified as N_1 have densities which are dominant above the dark Fermi level E_F while the states classified as N_2 have densities which are dominant below E_F, i.e., near and below midgap. These N_1 and N_2 states can have quite different carrier capture cross sections and can include more than one type of trapping or recombination center.

The occupation of the various states under illumination is shown schematicly in Fig. 6, where the presence of $\sigma_p \gg \sigma_d$ results in a large displacement of both the electron and the hole quasi-Fermi levels, E_{Fn} and E_{Fp}, from the thermal equilibrium E_F. The notation employed in this paper is that used by Rose[20]: the electron and hole recombination centers are p_r and n_r; the densities of all these centers are N_r, and the carrier capture cross sections are S_n and S_p. Because the relatively long electron lifetimes indicate that the densities of recombination centers are low enough to make any transition of electrons (and holes) between discrete centers highly unlikely the electron lifetime

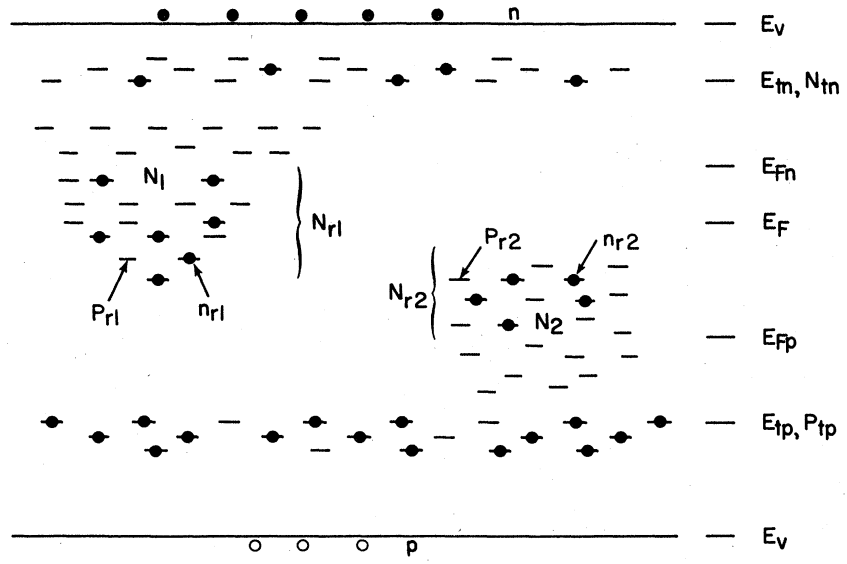

FIG. 6. Schematic energy-band diagram and distribution of states in a-SiH$_x$ (see text for details).

is given by

$$\tau_n = \frac{1}{v(S_{n1}p_{r1} + S_{n2}p_{r2})}, \tag{7}$$

where v is the thermal velocity of electrons and the subscripts 1 and 2 refer to the two classes of states in Fig. 6. The location of these recombination centers is defined by demarcation levels. Since these are closely coupled to the quasi-Fermi levels, to a good approximation they can be correlated with E_{Fn} and E_{Fp}.[20] (This approximation is only valid for results such as considered in this paper where E_{Fn} and E_{Fp} are significantly displaced from E_F). The displacement of E_{Fn} and E_{Fp} which results from increased illumination allow new states to act as recombination centers. The effect that the densities and capture cross sections of the p_r centers dominating the electron recombination have on τ_n and γ is expressed by Eq. (7). As a result extensive information can be obtained about the various states in the gap when E_{Fn} is swept over a wide energy range.

Although the occupation of the recombination centers is independent of their energy, being entirely determined by the electron-hole recombination traffic due to the absence of thermal reemission, this is not the case for the gap states which act as electron traps. Such states, which do not contribute to the recombination traffic, are occupied by localized electrons which are reexcited to the conduction band before they have an opportunity of recombining with localized holes. To a high degree of accuracy the density of such occupied states, $n_t(E)$, is given by

$$n_t(E) = N_t(E) \exp\left(\frac{(E - E_{Fn})}{kT}\right), \tag{8}$$

where $N_t(E)$ cm^{-3} is the density of the states at an energy E. It can be noted here that even though the τ_0 in Eq. (3) is determined by the occupancy of all the trapping states, including the large densities N_{tn}, for a continuous distribution of states to a good approximation $n_t = (kT/q)N_t(E_{Fn})$. This is due to the Boltzmann factor in Eq. (8) which makes the states close to E_{Fn} dominate n_t. This applies to deep states such as N_1 providing that the thermal emission rate of electrons from these states is greater than the rate at which the electrons are recombining, n/τ_n. Consequently, the values of τ_0 and n_t, as well as their dependence on f, also yield valuable information about the states in the gap which can be correlated in a self-consistent manner with the results obtained from the corresponding recombination kinetics. The various results presented in the preceding section are analyzed here in this manner.

The results in Fig. 1 indicate recombination characteristics dominated by deep-lying centers which are quite localized in energy. This is reflected by the independence of τ_n, which corresponds to constant value of the denominator in Eq. (8), as $E_c - E_{Fn}$ changes from 0.55 to 0.45 eV and E_{Fn} moves through the continuous distribution of N_1 states. The corresponding results for τ_0 and the constant value of $n_t = (kT/q)N_1(E_{Fn})$ indicate that E_{Fn} is displaced through a region of N_1 states which have a virtually constant density. The density of trapped electrons, $n_t = 6 \times 10^{15}$ cm^{-3}, corresponds to $N_1(E_{Fn}) \sim 10^{17}$ cm^{-3} eV^{-1}, a value that is in good agreement with those inferred from other measurements on similar films.[5] Also since $n \ll n_t$ these values of n_t indicate that the densities of p_{r2} states must be at least 10^{16} cm^{-3} if charge neutrality conditions are to be satisfied. This allows an estimate to be made for the electron capture cross sections of the N_1 states and the p_{r2} centers. Since the N_1 states in the vicinity of E_{Fn} determine τ_0, the emission of electrons from these states, ~0.5 eV from E_c, must be able to keep up with the recombination traffic. The minimum requirement for this is that S_{n1} be greater than 10^{-18} cm^2.[20] The estimate for S_{n2}, on the other hand, can be made from the fact that the N_1 states do not act as recombination centers so that Eq. (7) can be rewritten as $\tau_n = (vp_{r2}S_{n2})^{-1}$. Inserting $p_{r2} \sim 10^{16}$ cm^{-3} into this modified Eq. (7), a maximum value of less than 10^{-18} cm^2 is obtained for S_{n2} for the electron lifetimes of $5-8 \times 10^{-6}$ s in Fig. 1 and $v = 10^7$ cm s^{-1}. Such small values for electron capture cross sections are generally associated with acceptor-type centers which are negatively charged even when not occupied by a localized electron. (Because such centers have a Coulomb-attracting capture cross section for holes, they have a $S_p \gtrsim 10^{-13}$ cm^2).

The profound effect that recombination centers having very small electron capture cross sections have on the photoconductivity, electron lifetimes, and recombination kinetics has been discussed with reference to "electronic doping."[20] It was pointed out that in presence of $S_{n2} \ll S_{n1}$ there is a strong tendency for the S_{n2} centers to accumulate holes and become p_r centers. This results in a shift of electrons from the N_2 states to the N_1 states so that for $N_2 > N_1$ the N_1 states in Fig. 6 become occupied by electrons and $p_{r2} = N_{r1}$. Under such conditions τ_n becomes determined by p_{r2} states having a density N_{r1} so that Eq. (7) can be rewritten as

$$\tau_n = \frac{1}{vN_{r1}S_{n2}}. \tag{9}$$

It is important to note that in Eq. (9) the expres-

sion for τ_n contains the density N_{r1}, which is determined by the N_1 states, but that the electron capture cross section is S_{n2} which is that of an N_2 center. Furthermore, the presence of the S_{n2} centers reduces the role of N_1 states to that of electron traps or hole recombination centers even if the N_1 states are donor type having very large electron capture cross sections. This is consistent with the results of Fig. 1 just discussed where values of 10^{-18} cm^2 were obtained as a *lower* limit for S_{n1}. Two additional points can also be made here regarding the recombination kinetics. First, it is possible for the electron recombination not to be entirely dominated by the centers having these small values of S_{n2}, because in general the N_2 states can have different densities and types of recombination centers. This results in additional terms entering into the denominator of Eq. (9) and changing the kinetics. Second, at high levels of illumination a "saturation" of these S_{n2} centers can occur when the electron recombination ceases to be confined to these particular centers. Such transistions can lead to values of $\gamma < 0.5$ (Ref. 19) since a drastic decrease in τ_n can occur even when a small number of centers with large electron capture cross sections become involved in the recombination traffic.

The presence of these deep centers having $S_{n2} \ll S_{n1}$ is also consistent with the characteristics shown in Fig. 3 which illustrate a τ_n decreasing with f, a clear indication that the density of p_r recombination centers increases as E_{Fn} moves towards E_c. The changes in τ_n, which over many orders of magnitude of f exhibit a value of γ significantly different from 0.5 and 1, can be explained in terms of an exponential distribution of states above midgap.[20] Such a distribution of N_1 states can be represented as $N_1(E) = A\exp[-(E_c - E)/kT_1]$, where A is a constant and T_1 ($> T$) is a parameter which expresses how rapidly the densities change with energy. ($T_1 = T$ corresponds to a constant density of states). For this notation γ is given by $T_1/(T_1 + T)$. The results shown in Fig. 3, where $\gamma = 0.7$, reflect such an exponential distribution having $T_1 = 2.3$ and a τ_0 dominated by electrons trapped in the vicinity of E_{Fn}. However, the differences between τ_0 and τ_n indicate that the same class of states cannot act as both electron traps and recombination centers. As a result τ_n is given by Eq. (9), where due to the exponential nature of the N_1 the density $p_{r2} = N_{r1} \simeq kT_1 N_1(E_{Fn})$. This yields the relations characterizing the results in Fig. 3 which are

$$\tau_n = \frac{1}{vkT_1 N_1(E_{Fn}) S_{n2}} \propto f^{-(1-\gamma)}, \tag{10a}$$

and

$$\tau_0 = \left(\frac{n_t}{n}\right)\tau_n \simeq \frac{T}{vT_1 S_{n2} n} \propto f^{-\gamma}. \tag{10b}$$

The dependence of τ_n and τ_0 in Fig. 4 are in agreement with Eqs. (10a) and (10b). Applying these equations to the results obtained for τ_n, n and n_t yields a value of $\sim 10^{-19}$ cm^2 for S_{n2} (the electron capture cross section of the centers dominating the recombination) and a value of $\sim 10^{17}$ cm^{-3} eV^{-1} for $N_1(E_{Fn})$. Even though these τ_n, τ_0 characteristics are different from those of Fig. 1, they yield similar values for n_t and S_{n2}. Also in both cases the electron trapping has been dominated by the N_1 states, the densities of trapped electrons are less than 10^{16} cm^{-3} and there is no indication that they exceed the densities of p_r states. These characteristics correspond to positions of E_{Fn} sufficiently far away from E_{tn} so as to leave the majority of the N_{tn} states empty [Eq. (8)]. However, the results presented in Figs. 4 and 5, which exhibit transitions in photoconductivities from $\gamma > 0.8$ to $\gamma = 0.5$, indicate that sufficiently large displacements of E_{Fn} towards E_c obtained with temperature lead to recombination and trapping kinetics similar to those shown in Fig. 2. Although values of $\gamma = 0.5$ can be attributed to the presence of truly bimolecular recombination, i.e., direct recombination between either free or trapped carriers, such recombination is highly unlikely with the densities of carrier indicated by the results in Fig. 2. It has, however, been shown that $\gamma = 0.5$ can also be obtained when the density of trapped electrons begins to exceed p_r, the density of deep recombination centers occupied by holes.[20] Under these conditions the density of the $p_r = N_{r1}$ centers in Eq. (9) becomes modified to p', a value equal to the density of trapped electrons. Because of the continuous distribution of states it is very difficult to evaluate the exact density of trapped electrons; however, the results shown in Figs. 3, 4, and 6 clearly indicate that the transition to $\gamma = 0.5$ characteristics occur when E_{Fn} is close to the large density of N_{tn} states in Fig. 6. As a result characteristics such as shown in Fig. 2 can be associated with a density n_{tn} of electrons trapped in the N_{tn} states which are here approximated by an electron occupancy of a density of N_{tn} states at an energy $E_c - E_{Fn}$. By making $p'_r = n_{tn}$ and using Eqs. (1a), (1b), (3), (4), (8), and (10) the n, τ_n, and τ_0 of this regime are given by

$$n = \left(\frac{fN_c}{S_{n2}N_{tn}}\right)^{0.5} \exp\left(\frac{E_c - E_{tn}}{2kT}\right), \tag{11a}$$

$$\tau_n = \frac{1}{vS_{n2}n_t(E_{tn})} \propto f^{-0.5}, \tag{11b}$$

and

$$\tau_0 = \left(\frac{n_t}{n}\right)\tau_n = \tau_n\left(\frac{N_{tn}}{N_c}\right)\exp\left(\frac{E_c - E_{tn}}{kT}\right) \propto f^{-0.5}, \tag{11c}$$

where S_{n2} is still the electron capture cross section of the deep centers through which the free electrons recombine with the free holes. The transition to the above kinetics, from that determined solely by the occupation of the deep-lying states, depends on both the density of p_r states as well as N_{tn} and E_{tn}. As a result even with the same values of N_{tn} and E_{tn} transtions from $\gamma > 0.5$ to $\gamma = 0.5$ can occur at differnt positions of E_{Fn} when different densities of N_{t2} states (and p_r centers) are present in the films.

The results presented for the photoconductivities having $\gamma = 0.5$ are consistent with the relations shown in Eq. (11). For example, applying Eq. (11a) and (11b) to the results for the τ_n and τ_0 characteristics shown in Fig. 2, a value of $S_n \sim 10^{-19}$ cm^2 is obtained for the deep recombination centers. This is in very good agreement with the values obtained from the quite different τ_n, τ_0 characteristics shown in Figs. 1 and 4. In addition there is agreement between the values of $E_c - E_{tn} \sim 0.2$ eV obtained from electron drift mobility measurements,[3] and the activation energies of σ_p ($\gamma = 0.5$) shown here and those reported by Wronski and Carlson.[21] These activation energies of ~0.1 eV, quite different from the virtually temperature-independent $\sigma_p(\gamma = 0.9)$ in Fig. 3, are consistent with the $(E_c - E_{tn})/2$ given by Eq. (11a). There is also agreement between the kinetics discussed here and the transitions present between the photoconductivities having $\gamma > 0.5$ to those having $\gamma = 0.5$. These transition photoconductivities, σ_{TR}, correspond to a boundary condition where the electron lifetime satisfies both Eqs. (9) and (11). Since at this point the densities of recombination centers are $p_r = p_r' = N_t(E_{tn})$, the two equations yield σ_T as

$$\sigma_{TR} = q\mu_n\left(p_r\frac{N_c}{N_t}\right)\exp\left(-\frac{(E_c - E_{tn})}{kT}\right), \tag{12}$$

where p_r is the density of recombination centers unoccupied by electrons at the transition point. It can be seen from Eq. (12) that since σ_p depends on f, the values of σ_{TR} and the temperatures of the transitions depend on f as seen in Fig. 4. For p_r and μ_n, which are insensitive to temperature, Eq. (12) yields an activation energy, E_{TR}, for σ_{TR} which is equal to $E_c - E_{tn}$. The results obtained in Figs. 4 and 5 yield a value for $E_{TR} = E_c - E_{tn} \simeq 0.2$ eV. Since τ_n has some temperature dependence, a dependence which increases as γ deviates more from unity, the transition from region of $\gamma = 0.83$ to $\gamma = 0.5$ is not as clearly defined as that of $\gamma = 0.9$.

The expressions shown in Eqs. (11) and (12) can be used to estimate the densities of the shallow states, N_{tn}, and of the recombination centers from results such as presented in Figs. 2, 3, and 5. The constant ratio of 200 for τ_0/τ_n present in Fig. 2 gives a value of 200 for $(N_{tn}/kT)\exp[(E_c - E_{tn})/kT]$ [Eq. (11c)]. Thus for $E_c - E_{tn} = 0.2$ eV a value of $N_c/N_{tn} = 10$ is obtained which corresponds to a density $N_{tn} = 10^{19}$ cm^{-3} for $N_c = 10^{20}$ cm^{-3}. Although this is a large density of states, it is consistent with the draft mobility results and a microscopic free-electron mobility of 1 to 10 cm^2 V^{-1} s^{-1}. Although there is some uncertainty in the exact values of N_{tn}, Eq. (12) can be used to obtain the densities of p_r centers present in the transition photoconductivities, σ_{TR}. The values that are obtained from the results shown in Figs. 4 and 5 are $p_r < 10^{16}$ cm^{-3} and $p_r = 2$ to 3×10^{17} cm^{-3}, respectively. Such a large difference in the densities of the p_r centers is consistent with the significantly longer electron lifetimes (and larger photoconductivities) of the annealed film. It is also a clear indication that photoinduced recombination centers are introduced by the 200 mW/cm^2.[5] However, even in the case of the "short" electron lifetimes such as those shown in Fig. 1, the densities of these centers are still much smaller than N_{tn}.

This large difference between N_{tn} and the densities of recombination centers having $S_{n2} \simeq 10^{19}$ cm^2 has to be taken into account in the characterization of photoconductivities in which E_{Fn} is close to E_c and E_{tn}. Although the effects of other recombination processes and those due to holes trapped in the p_t states of Fig. 6 cannot be entirely discounted, the transitions observed in σ_p at the lowest temperatures in Fig. 3 can be readily accounted for by the "saturation" of the centers having $S_n \simeq 10^{-19}$ cm^2. At these low temperatures E_{Fn} can approach sufficiently close to E_{tn} to yield densities of electrons trapped in the N_{tn} states, $n_t(E_{tn}) = p_r'$, which approach those of all the centers having $S_{n2} \simeq 10^{-19}$ cm^2. When this occurs, the electron recombination paths can no longer be limited to only these centers so that a rapid decrease in τ_n occurs when E_{Fn} is further displaced which results in a low power dependence of σ_p on f.[19] The transitions in σ_p from a $\gamma = 0.5$ to a $\gamma \sim 0.4$ (and in the activation energy from ~0.1 to ~0.2 eV) present at the lower temperatures in Fig. 2 are consistent with the results on the densities of recombination centers that can be inferred from such a mechanism. For the same values of N_{tn} and E_{Fn} as those discussed above in the case of σ_{TR}, the densities obtained for the centers having $S_{n2} \simeq 10^{-19}$ are $\sim 5 \times 10^{17}$ cm^{-3}, which is consis-

tent with the lifetimes of $\sim 10^{-6}$ and Eq. (9). Because of the difficulties in characterizing the changes between the small values of γ, no attempt is made here to treat these transitions in detail. However, they are briefly discussed because such changes in γ are clearly not a low-temperature effect since they have also been observed on far-forward-biased Schottky barrier solar-cell structures at room temperature. Also, since they can be associated with the saturation of certain recombination centers, they are an indication of a regime in which the electron and hole lifetimes are approaching a common value.[19]

SUMMARY AND CONCLUSIONS

The photoconductivities of undoped discharge-produced a-SiH$_x$ films, deposited at substrate temperatures between ~200 and 300 °C, have been characterized in terms of electron trapping and recombination kinetics. These kinetics which over a wide range of illuminations and temperatures are consistent with free-carrier transport and the treatments extensively discussed by Rose, have been correlated with the states in the gap of the a-SiH$_x$ films. The recombination and electron lifetimes, which depend on the fabrication conditions and the thermal and optical exposure histories of the films, are found to be determined by the states located at and below midgap where at least two types of centers are present. The large photosensitivity, σ_p, and the long electron lifetimes, τ_n, found in these films result from low densities of gap states and recombination centers having an electron capture cross section, S_n, of $\sim 10^{-19}$ cm^2. The observed wide range of values for τ_n and σ_p can be explained by the differences in the densities of these centers and their effectiveness in counteracting the presence of states having much larger electron capture cross sections.

The different dependences of τ_n and σ_p on the intensity of illumination has been related to the recombination through the deep centers. The previously discussed[12,21] values of γ between 1.0 and 0.5, as well as those having values less than 0.5, have been correlated with the continuous distribution of gap states above midgap and the displacements of the quasi-Fermi levels E_{Fn}. The role of the states above midgap (and the dark Fermi level) is found to be limited to that of electron traps which in large part can be attributed to the presence of the centers having $S_n \sim 10^{-19}$ cm^2 and their role of "electronic dopants."[20] Consequently, not only the response-time characteristics but also the values of γ can be related to the densities and energy distributions of these states. The results obtained indicate that the densities of states in these films are $\sim 10^{17}$ cm^{-3} eV^{-1} in the region of ~0.6 to 0.35 eV from the conduction band E_c, and that for energies within 0.2 eV the densities are $N_{tn} \sim 0.1\, N_c \sim 10^{19}$ cm^{-3}. These large densities of shallow states are consistent with the results of electron drift mobility measurements on similar films. No evidence is found of the large peak in density of states at ~0.4 eV from E_c, a peak that has been extensively reported[9,11,28] for discharge-produced a-SiH$_x$ films. The absence of such a peak, however, is in agreement with the results reported by Hirose, Suzuki, and Doler[25] for their rf discharge-produced films. Our results also indicate the N_{tn} shallow states act as electron traps even down to temperatures of ~120 K and that the large densities of electrons present in these states at high levels of illumination and/or low temperatures only influence the kinetics of recombination through the deep-lying centers.

The reversible changes in the photoconductivity characteristics obtained with prolonged exposures to illumination are consistent with the introduction of photoinduced recombination centers deep in the gap. No effects were observed which could be attributed to changes in the states above midgap. Even though large decreases in τ_n occur, the changes in recombination kinetics are entirely consistent with an introduction of centers which have S_n significantly larger than $\sim 10^{-19}$ cm^2. Also the densities of these centers do not have to exceed values of 10^{16} to 10^{17} cm^{-3} eV, since in the films in which the largest changes have been observed ($\tau_n \sim 10^{-3}$ s) the densities of sensitizing centers are estimated to be in the low 10^{16}-cm^{-3} eV^{-1} range. The large role that free-carrier capture cross sections of recombination centers play in determining the carrier lifetimes allows such densities of states, which are $\sim 10^{-4}$ that of the hydrogen in the films,[29,30] to significantly affect the photoconductivity results. However, further detailed characterization of centers, such as discussed in this paper, is required before quantitative correlations can be made between the densities of states in a-SiH$_x$ films and theoretical models or structural defects present in the films.[31,32]

ACKNOWLEDGMENTS

The authors would like to thank D. E. Carlson and A. R. Triano for supplying the films, and T. D. Moustakas, A. Rose, D. L. Staebler, and R. Williams for helpful discussions. Research reported herein was prepared for the Department of Energy, Division of Solar Technology, under Contract No. EY-76-C-03-1286 and R. C. A. Laboratories, Princeton, New Jersey 08540.

*Present address: Exxon Research and Engineering Company, Corporate Research Laboratories, Linden, N.J. 07036

[1]R. C. Chittick, J. H. Alexander, and H. F. Sterling, J. Electrochem. Soc. 116, 77 (1969).
[2]P. G. LeComber, A. Madan, and W. E. Spear, J. Non-Cryst. Solids. 11, 219 (1972).
[3]D. E. Carlson and C. R. Wronski, J. Electron. Mater. 6, 95 (1977).
[4]C. R. Wronski, Proceedings of the Ninth Conference on Solid State Devices, Tokyo, 1977 [Jpn. J. Appl. Phys. Suppl. 17, (1) 299 (1978)].
[5]C. R. Wronski, IEEE Trans. Electron. Devices Ed-24, 351, (1972).
[6]D. E. Carlson and C. R. Wronski, Appl. Phys. Lett. 28, 671 (1976).
[7]D. E. Carlson, IEEE Trans. Electron Devices ED-24, 449, (1977).
[8]A. Madan, P. G. LeComber, and W. E. Spear, J. Non-Cryst. Solids 20, 239 (1976).
[9]P. G. LeComber, A. Madan, and W. E. Spear, J. Non-Cryst. Solids 11, 219 (1972).
[10]R. A. Street, J. C. Knights, and D. K. Biegelsen, Phys. Rev. B 18, 1880 (1978).
[11]R. J. Loveland, W. E. Spear, and A. Al-Shabarty, J. Non-Cryst. Solids 13, 55 (1973).
[12]P. J. Zanzucchi, C. R. Wronski, and D. E. Carlson, J. Appl. Phys., 48, 5227 (1977).
[13]D. A. Anderson and W. E. Spear, Philos. Mag. 30, 695 (1977).
[14]D. L. Staebler and C. R. Wronski, Appl. Phys. Lett. 31, 295 (1977).
[15]D. L. Staebler and C. R. Wronski, J. Appl. Phys., 51, 3262 (1980).
[16]C. R. Wronski, *Proceedings of the Thirteenth Photovoltaic Specialists Conference, Washington, D. C., 1978* (IEEE, New York, 1978), p. 744.
[17]I. Solomon, J. Dietle, and D. Kaplan, J. Phys. (Paris) 39, 1241 (1978).
[18]M. Tanielian, H. Fritzsche, C. C. Tsai, and E. Symbalisty, Appl. Phys. Lett. 33, 353 (1978).
[19]A. Rose, Phys. Rev. 97, 322 (1955).
[20]A. Rose, *Concepts in Photoconductivity and Allied Problems* (Interscience, New York, 1960).
[21]C. R. Wronski and D. E. Carlson, *Proceedings of the Seventh International Conference on Amorphous and Liquid Semiconductors, Edinburgh, 1977,* edited by W. E. Spear (CICL University of Edinburgh, Edinburgh, 1977), p. 452.
[22]C. R. Wronski, B. Abeles, G. D. Cody, D. Morel, and T. Tiedje, *Proceedings of the Fourteenth Photovoltaic Specialists Conference, San Diego, California, 1980* (IEEE, New York, 1980), p. 1057.
[23]A. R. Moore, Appl. Phys. Lett. 31, 762 (1977).
[24]C. R. Wronski, D. E. Carlson, and R. E. Daniel, Appl. Phys. Lett. 29, 602 (1977).
[25]M. Hirose, T. Suzuki, and G. H. Dohler, Appl. Phys. Lett. 34, 234 (1979).
[26]T. Tiedje, C. R. Wronski, and J. M. Cebulka, J. Non-Cryst. Solids 35–36, 743 (1980).
[27]C. R. Wronski, Sol. Energy Mater. 1, 287 (1979).
[28]H. Fritzsche, C. C. Tsai, and P. D. Persan, Solid State Technol. 21, 55 (1978).
[29]A. Triska, D. Denison, and H. Fritzsche, Bull. Am. Phys. Soc. 20, 392 (1972).
[30]M. H. Brodsky, M. Cardona, and J. J. Cuomo, Phys. Rev. B 16, 3556 (1977).
[31]A. J. Lewis, G. A. N. Connell, W. Paul, J. R. Pawlik, and R. J. Temkin, *Tetrahedrally Bonded Amorphous Semiconductors*, edited by M. H. Brodsky, S. Kirkpatrick, and D. Weaire (AIP, New York, 1974), p. 27.
[32]J. C. Knights, J. Non-Cryst. Solids 35–36, 119 (1980).